Influences of pi-pi Complex Formation, Dimerization, and Binding to Hemoglobin on the Planarity of Nickel(II) Porphyrins

ARTICLE *in* JOURNAL OF THE AMERICAN CHEMICAL SOCIETY · JANUARY 1990

Impact Factor: 12.11 · DOI: 10.1021/ja00158a030

3 AUTHORS, INCLUDING:

Mark R Ondrias
University of New Mexico
118 PUBLICATIONS **2,216** CITATIONS
SEE PROFILE

John A Shelnutt
University of Georgia
265 PUBLICATIONS **8,777** CITATIONS
SEE PROFILE

Influences of $\pi-\pi$ Complex Formation, Dimerization, and Binding to Hemoglobin on the Planarity of Nickel(II) Porphyrins†

R. G. Alden,‡ M. R. Ondrias,‡ and J. A. Shelnutt*,§

Contribution from the Department of Chemistry, University of New Mexico, Albuquerque, New Mexico 87131, and Fuel Science Division 6211, Sandia National Laboratories, Albuquerque, New Mexico 87185. *Received May 19, 1989*

Abstract: The effects of $\pi-\pi$ dimerization and complex formation on the planar and nonplanar conformations of the macrocycle of nickel(II) uroporphyrin I ($NiUroP^{8-}$) have been determined using Raman difference spectroscopy. Both planar and ruffled species, which coexist in alkaline solution, dimerize as evidenced by 1-3-cm^{-1} shifts to higher frequency in the structure-sensitive Raman lines with an apparent decrease in amount of the ruffled form of $NiUroP^{8-}$. Formation of the methyl viologen $\pi-\pi$ complex causes the uncomplexed planar form of $NiUroP^{8-}$ to ruffle slightly; the uncomplexed ruffled conformer of $NiUroP^{8-}$ also forms a complex with methyl viologen with a change in the apparent distortion. These two complexed ruffled forms are distinguished by the Raman marker lines, and both forms show evidence of the $\pi-\pi$ interaction between methyl viologen and the porphyrin macrocycle. These results are compared with similar resonance Raman data for nickel protoporphyrin reconstituted human hemoglobin, α-subunits of adult hemoglobin, and nickel protoporphyrin in cetyltrimethylammonium bromide (CTAB) micelles. The protein results show that the active site of the protein strongly favors the planar conformation of the macrocycle, more so in hemoglobin than in the α-subunits. The axial ligand affinity is lower for the ruffled macrocycle than for the planar form because the ruffled species is more coordinatively saturated as a result of its contracted metal core. As a result, the presence of a sizable ruffled component of four-coordinate nickel protoporphyrin in the α-chains accounts for their low affinity for the proximal histidine when compared to other Ni-reconstituted proteins with either the T or the R quaternary structure. This result suggests a possible mechanism for protein control of axial ligand affinity by modulation of the out-of-plane conformation of the porphyrin macrocycle.

Metalloporphyrin complexes play central roles in many catalytic processes in biological systems and in reactions of commercial interest.[1] In spite of their importance, the dependence of functional activities of the metalloporphyrins upon conformational distortion of the macrocycle has not been systematically investigated. Indeed, nonplanar (ruffled, domed, or flexed) conformations may influence many chemical and photochemical properties of porphyrins and have been proposed in biological systems to be important in the function of these prosthetic groups.[2-6] In heme proteins, for example, a protein-induced distortion of the porphyrin macrocycle might modify the chemical properties of the active site. Nonplanar distortions, such as doming of the macrocycle, have been observed in the X-ray crystal structures of some heme proteins.[5] As another example, the degree of ruffling of the tetrapyrrole macrocycle of cofactor F_{430} derivatives determines the axial ligand affinity of the Ni(II) atom in its core.[2-4] Protein control of macrocycle planarity of F_{430} may play a role in methylreductase activity. Finally, nonplanar conformational distortions of tetrapyrrole pigments of photosynthetic reaction centers have been suggested to control their photophysical properties.[6]

The metallouroporphyrins provide an interesting system for the investigation of weak interactions analogous to those between the macrocycle and the protein residues lining the binding site of the porphyrin moiety. These weak interactions can be modeled by self-aggregation[7-12] of the porphyrin and by $\pi-\pi$ complex formation with other organic molecules.[12-18] The uroporphyrins are unique in that, unlike other natural porphyrins, they do not aggregate in alkaline solution, except at high concentrations (>0.01 M). The lack of appreciable aggregation at high pH is attributable to electrostatic repulsions of the eight ionized acetic and propionic acid substituents at the β-carbon positions of the pyrrole rings. However, the uroporphyrins can be forced to dimerize at lower concentrations upon addition of salt, which shields the charges of the carboxylate groups.

Previous studies[7-12,14-18] have examined thoroughly the effects of the metal on the electronic structure of uroporphyrins and found that the metal plays a minor role in $\pi-\pi$ complex formation and aggregation. Indeed, $\pi-\pi$ complexes and aggregates are formed even for metal-free uroporphyrin. The induced changes in both the UV-visible absorption and the resonance Raman spectra are qualitatively similar regardless of the metal contained within the uroporphyrin core. For example, the Soret band exhibits marked broadening and a commensurate blue shift of 10-15 nm (depending on the metal derivative) upon aggregation. The α and β bands are also broadened but shift to a lesser degree to the red. Further, the spectral changes that result upon aggregation are similar irrespective of the method used to induce the process: addition of salt (~1 M), acidification, or high porphyrin concentrations.

* To whom correspondence should be addressed.

† This work was performed at Sandia National Laboratories and supported by the United States Department of Energy (Contract DE-AC04-76DP00789), the Gas Research Institute (Contract 5082-260-0767), and the National Institutes of Health (Grant GM33330).

‡ University of New Mexico.
§ Sandia National Laboratories.

(1) *The Porphyrins*; Dolphin, D., ed.; Academic: New York, 1978.
(2) Eschenmoser, A. *Ann. N.Y. Acad. Sci.* **1986**, *471*, 108.
(3) (a) Shelnutt, J. A. *J. Am. Chem. Soc.* **1987**, *109*, 4169. (b) Shelnutt, J. A. *J. Phys. Chem.* **1989**, *93*, 6283. (c) Crawford, B. A.; Findsen, E. W.; Ondrias, M. R. *Inorg. Chem.* **1988**, *27*, 1842.
(4) (a) Shiemke, A. K.; Scott, R. A.; Shelnutt, J. A. *J. Am. Chem. Soc.* **1988**, *110*, 1645. (b) Shiemke, A. K.; Kaplan, W. A.; Hamilton, C. L.; Shelnutt, J. A.; Scott, R. A. *J. Biol. Chem.* **1989**, *264*, 7276.
(5) (a) Takano, T. *J. Mol. Biol.* **1977**, *110*, 537. (b) Deatherage, J. F.; Loe, R. S.; Anderson, C. M.; Moffat, K. *J. Mol. Biol.* **1976**, *104*, 687. (c) Ladner, R. C.; Heidner, E. J.; Perutz, M. F. *J. Mol. Biol.* **1977**, *114*, 385.
(6) (a) Barkigia, K. M.; Chantraupong, L.; Smith, K. M.; Fajer, J. *J. Am. Chem. Soc.* **1988**, *110*, 7566. (b) Deisenhofer, J.; Epp, O.; Miki, K.; Huber, R.; Michel, H. *Nature* **1985**, *318*, 618.
(7) Blumberg, W. E.; Peisach, J. *J. Biol. Chem.* **1965**, *240*, 860.
(8) Shelnutt, J. A. *J. Phys. Chem.* **1984**, *88*, 4988.
(9) Shelnutt, J. A.; Dobry, M. M.; Satterlee, J. D. *J. Phys. Chem.* **1984**, *88*, 4980.
(10) Satterlee, J. D.; Shelnutt, J. A. *J. Phys. Chem.* **1984**, *88*, 5487.
(11) Satterlee, J. D.; Shelnutt, J. A. *Inorg. Chim. Acta* **1985**, *106*, 165.
(12) Shelnutt, J. A.; Dobry, M. M. *J. Phys. Chem.* **1983**, *87*, 3012.
(13) Mauzerall, D. *Biochemistry* **1965**, *4*, 1801.
(14) Shelnutt, J. A. *J. Am. Chem. Soc.* **1981**, *103*, 4275.
(15) Shelnutt, J. A. *J. Phys. Chem.* **1983**, *87*, 605.
(16) Shelnutt, J. A. *Inorg. Chem.* **1983**, *22*, 2535.
(17) Shelnutt, J. A. *J. Phys. Chem.* **1984**, *88*, 6121.
(18) Shelnutt, J. A. *J. Am. Chem. Soc.* **1983**, *105*, 7179.

0002-7863/90/1512-691$02.50/0

The nature of the metal also has little effect on the formation of $\pi-\pi$ complexes between metallouroporphyrins and many aromatic molecules such as methyl viologen[17] and phenanthroline derivatives.[15] The stacking interactions of the phenanthroline $\pi-\pi$ complexes are analogous to those occurring in the dimer. For the methyl viologen complexes, electrostatic interaction between charged groups on methyl viologen and on the uroporphyrin peripheral substituents also come into play. In all the $\pi-\pi$ complexes, the Soret band shifts by several nanometers to the red and the α and β also exhibit small spectral changes.

For the metallouroporphyrins, aggregation and $\pi-\pi$ complex formation compete with axial ligation. For example, metallouroporphyrins with ligands strongly bound in both axial positions of the metal do not easily form either $\pi-\pi$ complexes or aggregates,[18] while metals that add only one axial ligand dimerize and form 1:1 complexes. Metallouroporphyrins with no axial ligands from 2:1 $\pi-\pi$ complexes with aromatic molecules and, also, form acid aggregates larger than dimers. In some cases where axial ligands are only weakly bound, aggregation and $\pi-\pi$ complex formation occur and result in displacement of the weakly bound ligand.[12] Thus, aggregation and complex formation can influence the coordination number. It is also possible that aggregation and $\pi-\pi$ complex formation perturb the planarity of the macrocycle, which in turn can affect other properties such as axial ligand affinity and redox potential.

In the present work we have used $\pi-\pi$ complexation and dimerization to mimic the weak interactions that a porphyrin macrocycle might experience in the active site of an enzyme. In particular, we have examined the effects of dimerization and $\pi-\pi$ complex formation with methyl viologen (MV^{2+}) on the macrocycle conformation of nickel(II) uroporphyrin I ($NiUroP^{8-}$). We present a detailed study of $NiUroP^{8-}$ and $CuUroP^{8-}$ using Raman difference spectroscopy (RDS) to determine the nonplanar conformations of the macrocycle. Monomeric $NiUroP^{8-}$ in solution displays behavior consistent with a conformational equilibrium between a S_4 symmetry ruffled conformer and a more planar conformation, in analogy to nickel octaethylporphyrin (NiOEP).[19,20] Nickel porphyrins tend to exhibit ruffled macrocycles because the unconstrained Ni–N bond distance is smaller than the optimum porphyrin core size. Under similar conditions, $CuUroP^{8-}$ exhibits only the planar conformation because the unrestrained Cu–N bond distance is larger than the Ni–N bond distance and closer to the optimum core size, so there is no reason for $CuUroP^{8-}$ to ruffle. We find that dimerization of $NiUroP^{8-}$ influences the equilibrium between the ruffled and the planar form. MV^{2+} forms $\pi-\pi$ complexes with both the planar and the ruffled $NiUroP^{8-}$ species. The resonance Raman spectra reveal that both species are affected by $\pi-\pi$ interaction between MV^{2+} and the porphyrin macrocycle. In addition, the uncomplexed planar species becomes ruffled in the complex. The conformation of the uncomplexed ruffled species also appears to become more ruffled upon MV^{2+} binding.

Replacement of the iron protoporphyrin of native hemoglobin with nickel protoporphyrin, which like NiOEP and $NiUroP^{8-}$ has a ruffled component in solution, influences the conformation of the nickel porphyrin macrocycle. We find that the protein environment forces the nickel protoporphyrin macrocycle into a planar conformation in hemoglobin. However, Ni reconstitution of the isolated α-subunits of hemoglobin appears only to reduce the degree of ruffling. The presence of a ruffled component in the Ni α-chains may account for the lower affinity for proximal histidine observed for the α-subunits when compared with the intact nickel hemoglobin tetramer.

Materials and Methods

The metal derivatives of uroporphyrin I (alternating acetic and propionic acid groups at the eight β-carbons of the pyrrole rings) were obtained from Porphyrin Products (Logan, UT) and were used without further purification. Resonance Raman data were obtained on a difference spectrometer previously described.[15] Samples of the metallouroporphyrin ($\sim 5 \times 10^{-5}$ M) in 0.1 M KOH were added to one side of a partitioned cell, while either dimerized metallouroporphyrin (5×10^{-5} M) or metallouroporphyrin complexed with MV^{2+} was added to the chamber on the other side of the rotating cell. Dimerized $MUroP^{8-}$ was formed by saturating the solution with KCl (~ 5 M). MV^{2+} complex was made by adding solid MV^{2+} to a solution of monomeric $NiUroP^{8-}$. The MV^{2+} concentration was 1×10^{-3} M.

The partitioned cell is spun at 50 Hz, which enables the two samples to be probed alternately by the laser radiation and also prevents heating. Simultaneous collection of the spectra of the two samples allows for elimination of errors resulting from variations in instrument response and grating positioning. Laser excitation at 413.1 nm from a krypton ion laser was used.

The two Raman spectra are stored in computer memory and subsequently modeled[21] using both Voigt and Lorentzian line shapes to fit the Raman spectra using up to eight lines. Least-squares fitting determines the position and line width of the peaks present in the spectra. A sloped linear base line and the percent Gaussian contribution to the line are also treated as parameters in the least-squares fitting procedure. However, the fits shown are with pure Lorentzian line shapes.

Molecular modeling calculations were carried out on a MicroVAX II host computer and visualized using an Evans & Sutherland PS390 graphics terminal. The energy-minimized structures were obtained by several successive 30-ps dynamics runs in which the temperature was decreased from 300 to 0 K in 3 ps, followed by energy optimization. BIOGRAF software (BioDesign) and DREIDING force field parameters (Mayo, S. L.; Olafson, B. D.; Goddard, W. A., III, BioDesign, Inc., to be published) were used for the molecular mechanics calculations. Force field parameters for nickel (stretching force constant = 200 (kcal/mol)/Å^2, Ni–N equilibrium bond distance = 1.85, nonbonding radius = 2.27 Å, and depth of van der Waals potential energy = 0.055 kcal/mol) were determined by comparison of predicted and X-ray crystal structures.

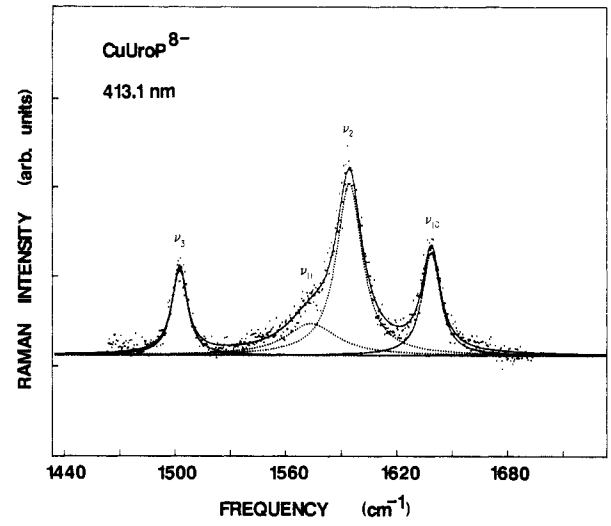

Figure 1. Lorentzian decomposition of the resonance Raman spectrum of $CuUroP^{8-}$ in 0.1 M KOH.

Results

Figure 1 shows the resonance Raman spectra of the $CuUroP^{8-}$ monomer obtained with 413.1-nm excitation. Systematic shifts to lower frequency relative to monomeric $CuUroP^{8-}$ are observed (not shown) in the methyl viologen complex[15,17] with $CuUroP^{8-}$. Shifts to higher frequency are observed for the $CuUroP^{8-}$ dimer.[9] Absorption spectral changes also accompany dimerization and complexation, and these have been interpreted in terms of shifts in the frontier orbitals of the macrocycle.[9,17,22] For example, a blue shift (398 → 382 nm) in the Soret band occurs upon dimerization, while a red shift (398 → 405 nm) accompanies formation of the MV^{2+} complex.

As can be seen in Figure 1, no shoulders or other evidence of multiple conformations are present in the spectra of $CuUroP^{8-}$.

(19) Alden, R. G.; Crawford, B. A.; Doolen, R.; Ondrias, M. R.; Shelnutt, J. A. *J. Am. Chem. Soc.* **1989**, *111*, 2070.
(20) Brennan, T. D.; Scheidt, W. R.; Shelnutt, J. A. *J. Am. Chem. Soc.* **1988**, *110*, 3919.
(21) Stump, R. F.; Deanin, G. G.; Oliver, J. M.; Shelnutt, J. A. *Biophys. J.* **1987**, *51*, 605.
(22) Shelnutt, J. A.; Ortiz, V. *J. Phys. Chem.* **1985**, *89*, 4733.

Table I. Frequencies (cm^{-1}) of the Core-Size Marker Lines for $CuUroP^{8-}$ and $NiUroP^{8-}$ and Their Salt Dimers and Methyl Viologen Complexes[a]

mode	frequency			line width			relative areas		
	monomer	dimer	MV^{2+}	monomer	dimer	MV^{2+}	monomer	dimer	MV^{2+}
				$NiUroP^{8-}$					
ν_4, ν_4'	1383	1384	1381						
ν_3'	1518.0 ± 0.4	1520.3 ± 0.7		13 ± 3	11 ± 4		2.6	1.4	
	1517.4 ± 0.4[b]			**13 ± 4**			**1.5**		
ν_3	1523.3 ± 0.2	1525.0 ± 0.3		8 ± 3	7 ± 4		1.0	1.0	
	1522.7 ± 0.3		**1516.2 ± 0.1**	**10 ± 4**		**12 ± 2**	**1.0**		**1.0**
ν_2, ν_2'	1602.8 ± 0.1	1605.4 ± 0.1		20 ± 3	19 ± 4				
	1599.2 ± 0.1		**1597.6 ± 0.1**	**21 ± 4**		**17 ± 3**			
ν_{10}'	1651.1 ± 0.5	1649.9 ± 3.8		18 ± 6	34 ± 22		2.5	0.9	
	1651.9 ± 0.7		**1647.0 ± 0.6**	**21 ± 7**		**14 ± 6**	**1.0**		**0.7**
ν_{10}	1661.1 ± 0.2	1661.9 ± 0.2		13 ± 4	13 ± 6		1.0	1.0	
	1661.3 ± 0.3		**1654.7 ± 0.3**	**12 ± 5**		**11 ± 4**	**1.0**		**1.0**
				$CuUroP^{8-}$[c]					
ν_4	1379	1380	1377	14 ± 2					
ν_3	1500	1503	1498	10 ± 3	7 ± 3				
ν_2[d]	1593	1594		17 ± 4	18 ± 4				
ν_{10}	1637	1640	1636	11 ± 1	12 ± 1				

[a] Confidence limits are obtained from the correlation matrix of the least-squares fits. [b] Bold and regular type faces indicate spectral data, which were obtained in pairs using the Raman difference spectrometer. Bold type gives the data for one pair of spectra; regular type gives data for the other pair. [c] Taken from ref 9, 15, and 17. [d] Present work.

Curve fitting with Lorentzian (or Voigt) line shapes yields converged fits with frequencies for ν_3, ν_2, and ν_{10} at 1500, 1593, and 1637 cm^{-1}, respectively. Line widths were typical of many other planar metalloporphyrins. Analogous single-component fits are also found in both the dimerized and π–π complexed $CuUroP^{8-}$ spectra (see Table I). These spectra are not shown, since they are virtually identical with the one shown in Figure 1 except for small frequency shifts. The Raman lines noted are well characterized as markers of the center-to-nitrogen(pyrrole) distance or core size of *planar* metalloporphyrins[23] but were recently shown to be indicators of ruffled conformations coexisting with planar forms in solution.[19,20]

The Raman data for $NiUroP^{8-}$ taken with 413.1-nm excitation are shown in Figure 2. Table I lists the frequencies and other spectral parameters determined from the least-squares fits for the structure-sensitive marker lines. Shifts and line-shape changes are observed upon dimerization and complexation for ν_4, ν_3, ν_2, and ν_{10}, relative to the frequencies found for the respective modes in the isolated species.[17] However, curve fitting shows that additional lines are present in all three spectra shown in Figure 2 on the low-frequency sides of the core-size marker lines. The low-frequency components of these lines in the monomeric $NiUroP^{8-}$ solutions are near 1518, ~1595, and 1652 cm^{-1} and are referred to in Table I as ν_3', ν_2', and ν_{10}', respectively. (Curve-fitting in the region of ν_2 is problematic because of overlap with several other lines, such as ν_{11} at ~1570 cm^{-1}. Consequently, only two Lorentzian lines were assumed to simulate the spectrum between 1560 and 1630 cm^{-1}, and only the shift in the line near 1600 cm^{-1}, which is composed primarily of ν_2 and ν_2' is considered significant.)

The changes in relative intensities, line widths, and positions of the two components of each line account for the apparent line-shape changes noted upon dimerization.[9] The high-frequency components ν_3 and ν_{10} shift to higher frequency upon dimerization by 1–2 cm^{-1} as has been observed for other metallouroporphyrins.[9] Shifts of similar magnitude may occur for ν_3', ν_2', and ν_{10}'; however, the calculated shifts are not statistically significant based on the confidence levels obtained from the fitting procedure.

Upon complexation of MV^{2+} and $NiUroP^{8-}$, ν_{10}' shifts to 1647 cm^{-1}. The lines ν_3' and ν_2', however, are not discernable. Complexation of MV^{2+} with $NiUroP^{8-}$ shifts both ν_3 and ν_{10} by about −7 cm^{-1} relative to the monomeric form. The shift for ν_3 is apparently larger than for ν_3', so that the separation of the two components is decreased and they cannot be resolved reliably by the fitting procedure. Table II lists the shifts in the core-size marker lines of the salt dimer and MV^{2+}–$NiUroP^{8-}$ complex relative to monomeric $NiUroP^{8-}$. Also, the shifts of the core-size markers are given for the $CuUroP^{8-}$ dimer and methyl viologen complex for comparison.

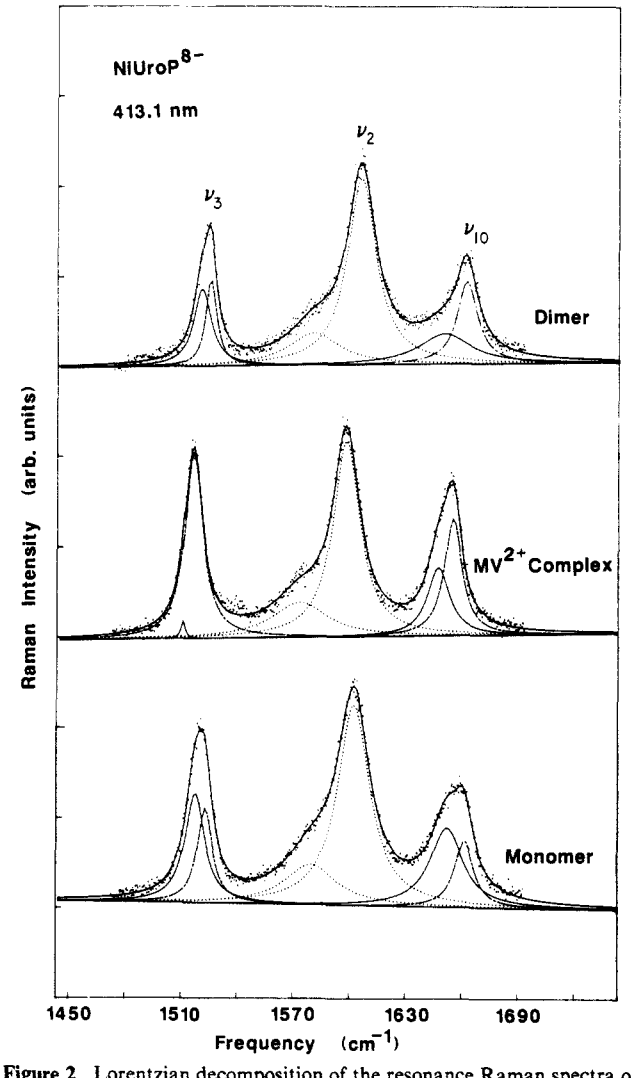

Figure 2. Lorentzian decomposition of the resonance Raman spectra of $NiUroP^{8-}$ in 0.1 M KOH (bottom), (center) with added methyl viologen and (top) saturated with KCl.

(23) (a) Spaulding, L. D.; Chang, C. C.; Yu, N.-T.; Felton, R. H. *J. Am. Chem. Soc.* **1975**, *97*, 2517. (b) Parthasarathi, N.; Hansen, C.; Yamaguchi, S.; Spiro, T. G. *J. Am. Chem. Soc.* **1987**, *109*, 3865.

Table II. Frequency Shifts[a] for the Planar and Ruffled Components of ν_3, ν_2, and ν_{10} That Occur upon Dimerization and Methyl Viologen Complex Formation[b]

	CuUroP^{8-}		NiUroP^{8-}	
mode	$\Delta\nu_{dimer}$[c]	$\Delta\nu_{MV^{2+}}$[d]	$\Delta\nu_{dimer}$[e]	$\Delta\nu_{MV^{2+}}$[e]
ν_4, ν_4'	2.1	−2.4	1.2 ± 0.4	−2.6 ± 0.4
ν_3'			2.3 ± 1.1	
ν_3	2.9	−2.2	1.7 ± 0.5	−6.7 ± 0.4
ν_2, ν_2'	0.8[e]		2.6 ± 1.1	−4.6 ± 0.2
ν_{10}'			−1.2 ± 4.3	−4.9 ± 1.4
ν_{10}	2.9	−1.3	0.8 ± 0.4	−6.6 ± 0.6

[a] Relative to the monomer. [b] Confidence limits obtained from the curve fitting procedure are shown as errors. [c] Taken from ref 9. [d] Taken from ref 17. [e] Present work.

The current Raman results suggested that a reanalysis of some of our previous[24,25] Raman data for nickel protoporphyrin reconstituted hemoproteins was necessary. Figure 3 shows the resonance Raman spectrum of nickel-reconstituted human hemoglobin A (NiHbA). NiHbA contains both four-coordinate sites and five-coordinate sites with the proximal histidine as the fifth ligand. In the spectrum of four-coordinate NiProtoP^{2-} in cetyltrimethylammonium bromide (CTAB) micelles, shown for comparison in Figure 3, both planar and ruffled conformers are clearly evident. The frequencies of ν_{10}' and ν_3' of NiProtoP^{2-} are shifted from those of the planar conformer by 6.3 ± 0.9 and 4.6 ± 0.5 cm^{-1}, as expected for a ruffled conformer. As is the case for NiUroP^{8-} and NiOEP, the line widths for the ruffled conformer (15 ± 6 and 11 ± 4 cm^{-1} for ν_{10}' and ν_3') are larger than those for the planar form (8 ± 4 and 7 ± 3 cm^{-1}). None of the ruffled component is detected for NiHbA; however, Ni α-chains do exhibit ruffling. The data for the Ni-reconstituted proteins is summarized in Table III.

Discussion

Core-Size and Ruffling Distortions of Nickel Porphyrins. The frequencies of the Raman lines above 1450 cm^{-1}, particularly ν_3, ν_2, and ν_{10}, have been shown to display an inverse linear correlation with the core size for *planar* metalloporphyrins with a variety of metals, including Ni, Cu, Fe, and Mn.[23] The core-size marker lines are insensitive to peripheral substituent effects. Alden et al.[19] found that these modes are also sensitive to the degree of nonplanarity exhibited by the ruffled macrocycle in solution. Both the planar and nonplanar forms coexist in solution. The ruffled component of NiOEP in solution was found to have shifts in ν_3, ν_2, and ν_{10} of −5, −7, and −11 cm^{-1}, respectively, relative to the frequencies of the planar form in NiOEP.

The relative magnitudes of the ruffling-induced shifts are distinct from the relative magnitudes observed for core-size changes, so that a ruffling distortion can be distinguished from a core-size distortion. Further, the ruffling shifts do not predict either the direction or the magnitude of the change in core size for the *ruffled* structure. It is apparent, therefore, that the nominally core-size-dependent lines above 1450 cm^{-1} are also affected by conformational heterogeneity resulting from the existence of low-energy nonplanar conformations. Another line, ν_4, at 1383 cm^{-1} for NiOEP is relatively insensitive to core size and ruffling but is dependent on oxidation state and other influences upon macrocycle π-charge density.[26] The shifts of the ruffled form in solution (−5 and −11 cm^{-1} for ν_3 and ν_{10}, respectively) are somewhat smaller than, but *proportional* to, the shifts exhibited by the S_4 ruffled tetragonal crystalline form relative to the planar triclinic forms (−11- and −21-cm^{-1} shifts relative to ν_3 and ν_{10} of the B form).[20,23] For example, the ruffling shift for ν_{10} is roughly twice the shift in ν_3 for both the solution and crystal species. The shifts in these two lines are more nearly equal for the core-size pattern of marker line shifts.

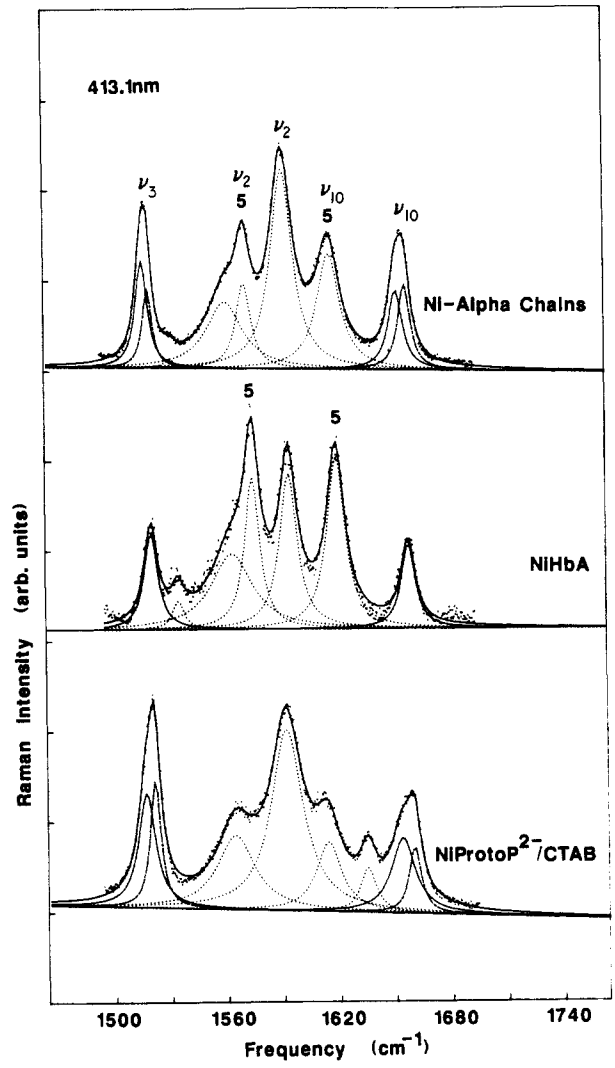

Figure 3. Lorentzian decomposition of the resonance Raman spectra of (bottom) nickel protoporphyrin in cetyltrimethylammonium bromide micelles in 0.1 M NaOH, (center) nickel hemoglobin 0.05 M phosphate buffer at pH 7.5, and (top) Ni-reconstituted α-subunits. The lines labeled by 5's indicate the Raman lines of the five-coordinate sites of NiHbA.

If the ruffling dihedral angle (pyrrole twist angle) is assumed to be proportional to the core-size shifts, then we can give an estimate of the ruffling angle of the macrocycle in various environments. The estimate can be based on the known shifts and ruffling angle for the NiOEP crystals. For example, ν_{10} shifts by −21 cm^{-1} for the crystal dihedral angle of 32.8°,[27] or 1.6° per wavenumber. Thus, the average dihedral angle for the ruffled solution forms of NiOEP is estimated to be 11 × 1.6 = 17°. Nevertheless, this method of estimation of the out-of-plane distortion relies on the linearity assumption, which probably gives an upper limit for the ruffling angle.

The conformational heterogeneity of nickel porphyrins results from a novel tradeoff between energetic considerations. The nickel ion is small and favors a highly contracted core with optimum Ni–N distances of about 1.85 Å. Thus, nickel bonding to the equatorial porphyrin ligand prefers a ruffled macrocycle conformation, which allows a closer approach of the pyrrole nitrogens and results in a more coordinatively saturated Ni ion. On the other hand, the conjugated bonding of the macrocycle skeleton favors a planar conformation but results in much longer than optimal Ni–N bond distance and hence a less coordinatively saturated Ni ion. Apparently, the net result of these opposing energetic contributions is that the planar and ruffled conformers

(24) Shelnutt, J. A.; Alston, K.; Ho, J.-Y.; Yu, N.-T.; Yamamoto, T.; Rifkind, J. M. *Biochemistry* **1986**, *25*, 620.
(25) Shelnutt, J. A.; Findsen, E. W.; Ondrias, M. R.; Alston, K. *ACS Symp. Ser.* **1987**, *No. 344*, Chapter 24.
(26) (a) Yamamoto, T.; Palmer, G.; Gill, D.; Salmeen, I. T.; Rimai, L. *J. Biol. Chem.* **1973**, *248*, 5211. (b) Spiro, T. G.; Strekas, T. C. *J. Am. Chem. Soc.* **1974**, *96*, 338. (c) Spiro, T. G.; Burke, J. M. *J. Am. Chem. Soc.* **1976**, *98*, 5482.
(27) Cullen, D. L.; Meyer, E. F. *J. Am. Chem. Soc.* **1974**, *96*, 2095.

Table III. Frequencies (cm^{-1}) and Other Spectral Parameters for Structure-Sensitive Lines of the Four-Coordinate Sites of Nickel-Reconstituted Globins[a]

	frequency			line width			relative areas		
mode	NiProtoP^{2-}	NiHbA	Ni α-chain	NiPP	NiHbA	Ni α-chain	NiPP	NiHbA	Ni α-chain
ν_4, ν_4'	1378[b]								
ν_3'	1514.8 ± 0.4			11 ± 4			1.5		
			1516.6 ± 0.3[c]			**8 ± 2**			**1.7**
ν_3	1519.4 ± 0.1	1518.6 ± 0.1		7 ± 3	9 ± 3		1.0		
		1518.4 ± 0.1	**1519.6 ± 0.3**		**8 ± 2**	**6 ± 3**			**1.0**
ν_2, ν_2'	1589.8 ± 0.1	1592.3 ± 0.1		20 ± 4	11 ± 3				
		1592.3 ± 0.1	**1590.8 ± 0.1**		**11 ± 2**	**14 ± 2**			
ν_{10}'	1651.6 ± 0.7			15 ± 6			2.2		
			1652.5 ± 0.3			**9 ± 3**			**1.1**
ν_{10}	1657.9 ± 0.2	1657.3 ± 0.1		8 ± 4	9 ± 3		1.0		
		1656.1 ± 0.1	**1657.2 ± 0.2**		**9 ± 2**	**8 ± 3**			**1.0**

[a] The errors indicated represent confidence levels for the least-squares fits, not true errors. [b] Taken from ref 24. [c] Bold and regular type faces indicate spectral data, which were obtained in pairs using the Raman difference spectrometer. Bold type gives the data for one pair of spectra; regular type gives data for the other pair.

are similar in energy and thus are in dynamic equilibrium.

NiUroP^{8-}, in analogy with NiOEP, also displays planar and nonplanar conformations in solution as evidenced by our decomposition of the Raman lines, ν_3 and ν_{10}, into two components each (Figure 2). The ν_3' and ν_{10}' lines are shifted by −5 and −10 cm^{-1} from the corresponding lines (ν_3 and ν_{10}) of the planar form (see monomer data in Table I) and thus are similarly assigned to the S_4 ruffled conformer. The estimated average dihedral angle for the ruffled component (16°) is about the same as noted for NiOEP. Further, the line widths of the ruffled form are in every case broader than those of the planar form. This result implies that multiple conformations (e.g., multiple degrees of S_4 ruffling) coexist in dynamic equlibrium in solution, generating a broad ensemble of distinct frequencies for the ruffled components with the calculated center frequencies listed in Table I. In contrast, the Raman lines of the planar species exhibit the widths (8–14 cm^{-1}) observed for other metalloporphyrins in solution.

Effects of Dimerization on Macrocycle Conformation. The shifts in the Raman core-size marker lines (see Tables I and II) and UV–visible absorption bands clearly show that dimerization and π–π complex formation produce different effects on the electronic and structural characteristics of metallouroporphyrins.[7-18] The pattern of Raman shifts observed upon dimerization (roughly equal shifts for ν_4, ν_3, and ν_{10}) deviates significantly from the core-size and ruffling patterns of shifts. Moreover, the shifts to high frequency that occur upon dimerization are roughly comparable for the planar and ruffled species (although the determined shifts for the ruffled form are not statistically significant). Thus, it appears that both planar and nonplanar species are affected similarly by dimerization.

The increases in frequency of the marker lines observed for the planar forms (+1.7 ± 0.5 and +0.8 ± 0.4 cm^{-1} for ν_3 and ν_{10}, respectively) are within errors consistent with dimerization. Similar increases (1–3 cm^{-1}) in the marker line frequencies are observed for other metallouroporphyrin dimers.[9] The behavior of CuUroP^{8-} is typical of this phenomenon (Table II). These shifts are caused by a decrease in macrocycle π-charge density.[8,20] A core-size decrease also results from the π–π interactions between stacked porphyrin macrocycles in the dimer. A similar increase in marker line frequencies is observed when the triclinic crystalline forms of NiOEP are compared.[20] The triclinic crystals differ in that NiOEP molecules of the triclinic B form are stacked in a manner that permits π–π interaction, whereas in the triclinic A form they cannot. The small decrease in core size predicted by the increase in marker line frequencies is observed in the crystal structures.

In addition, it is apparent from the spectra shown in Figure 2 that the equilibrium between the ruffled and planar forms of NiUroP^{8-} is affected by addition of salt to the solution, i.e., by dimerization. This conclusion is based upon the low integrated intensities of the lines of the ruffled form in saline solution (see relative areas in Table I). Clearly, care must be exercised in using the areas of the Raman peaks as an indication of the relative populations of the nickel porphyrin conformers because of the large errors in curve fitting and differences in Raman scattering resonance-enhancement conditions. The latter problem is a result of the monomeric, dimeric, and π–π complexed NiUroP^{8-} species having different Soret absorption maxima at 391, 377, and 399 nm, respectively. The 413.1-nm excitation wavelength used in the Raman experiments is in preresonance with the Soret bands of all three species and far from the α and β bands as well. A reasonable assumption is that the slopes of the tails of the absorption bands of the monomeric planar and ruffled forms do not change significantly at 413.1 nm upon dimerization or complexation. Thus, although the absolute intensities may change upon formation of the dimer or complex, the relative intensities of the planar and ruffled conformers should be qualitatively representative of the changes in populations of the two conformers.

The findings for the dimer demonstrate that the local environment plays an important role in determining the conformation of the porphyrin macrocycle. The converse may also be true. Previous studies have found the binding energy of the metallouroporphyrin dimers to be lower for NiUroP^{6-}Na$_2$ (11 kcal/mol) than for CuUroP^{6-}Na$_2$ (12 kcal/mol).[9] (The ΔG_4's for dimerization are for 5.5 M salt at which concentration and neutralization of two of the eight carboxylates of each porphyrin occurs. ΔG_4 is calculated using the parameters determined in ref 9.) The decreased binding energy for NiUroP^{8-}, compared with another four-coordinate metallouroporphyrin, CuUroP^{8-}, may be a result of the conformational equilibrium between planar and ruffled species that comes into play for NiUroP^{8-}.

Effects of Methyl Viologen π–π Complex Formation on Macrocycle Conformation. The addition of methyl viologen to a solution of a metallouroporphyrin results in a strong π–π complex. The strength is due to electrostatic interaction of the carboxylate substituents of the uroporphyrin octaanion and the positive charges at opposite ends of the methyl viologen dication. Interestingly, the shifts in ν_4, ν_3, ν_2, and ν_{10} for the complex relative to the monomer are to lower frequency, the opposite direction of the shifts for the dimer. The pattern of shifts in the core-size and oxidation-state marker lines is consistent with an increase in the π-charge density in the macrocycle.

Upon addition of MV^{2+} to a monomeric solution of NiUroP^{8-} the modes indicative of the uncomplexed ruffled and planar species shift to low frequency. Because both uncomplexed conformers exhibit shifts in the Raman peak positions upon MV^{2+} binding, both forms must be interacting with MV^{2+} in a π–π complex (i.e., MV^{2+} forms a π–π complex with both conformers giving two conformationally distinct types of complexed ruffled species). In fact, the shift $\Delta\nu_{10}'$ for the uncomplexed ruffled species is comparable to or larger than the shift found for other metallouroporphyrin–MV^{2+} complexes.[17] The shifts for the marker lines ν_3 and ν_{10} of NiUroP^{8-} are also larger than expected for a planar MV^{2+}–metallouroporphyrin complex (Table II). The shift in the oxidation-state marker line, which is composed of both ν_4 and ν_4' for NiUroP^{8-}, exhibits only the 2–3-cm^{-1} shift expected for the

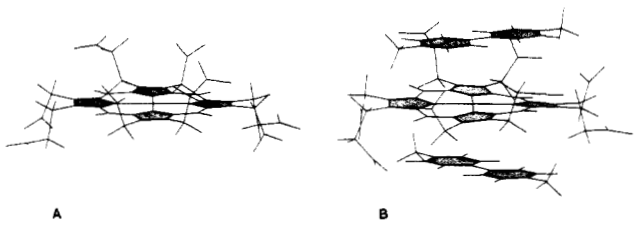

Figure 4. Structure of (A) isolated nickel uroporphyrin and (B) the methyl viologen–nickel(II) uroporphyrin complex calculated using modified Dreiding force field and a dielectric constant of 78. Result of dynamics calculation in which the temperature is lowered from 300 to 0 K in 30 ps followed by energy minimization.

complex. The Raman results can be explained if the MV^{2+} complex favors ruffled forms, that is, if binding MV^{2+} to $NiUroP^{8-}$ forces the uncomplexed planar form to ruffle. In this case, the frequencies of ν_3, ν_2, and ν_{10} would be lowered more than the 1–3 cm^{-1} expected as a result of the π–π interaction alone, and the shift in ν_4 would be in the 1–3-cm^{-1} range as observed. Using 1.6° per cm^{-1}, the dihedral angle of the new ruffled form is estimated to be $5 \times 1.6 = 8°$. The uncomplexed species that is ruffled appears to ruffle to a greater extent upon complex formation. Finally, we note that the relative integrated intensity of ν_{10}' of the complex is lower than that for ν_{10}' of the monomer.

It might be supposed that the MV^{2+}-induced ruffling of the macrocycle may result from the twist in the bond between the pyridinium rings of methyl viologen. However, molecular mechanics calculations predict this torsion angle to be only 3° in the energy-minimized MV^{2+} structure. Molecular mechanics calculations performed on the $NiUroP^{8-}$ complex with two MV^{2+} molecules suggest that the macrocycle is ruffled in its minimum energy configuration. The energy-minimized structures of $NiUroP^{8-}$ and the complex are shown in Figure 4. The N–Ni–N dihedral angle (i.e., the twist angle between the planes of opposite pyrrole rings) that expresses the degree of ruffling is found to be between 8 and 12° for the complex but less than 2° for isolated $NiUroP^{8-}$. MV^{2+} in the complex has a smaller dihedral angle between the pyridinium rings in the complex (~1°) than for isolated MV^{2+}. It is doubtful that the MV^{2+} torsion angle gives rise to the ruffling, but rather the orientations of the two MV^{2+} molecules across opposite methine bridges are the important factor.

It might also be noted that $CuUroP^{8-}$ does not ruffle significantly in the complex, since the shifts in ν_3, ν_2, and ν_{10} are small and approximately equal (Table II). Thus, the complex-induced ruffling of $NiUroP^{8-}$ is a consequence of the general tendency of nickel porphyrins to ruffle.

Even though the methyl viologen–metallouroporphyrin complexes have lower binding energies (7.0–8.0 kcal/mol) than the dimer, the structural perturbations imposed by MV^{2+} binding to $NiUroP^{8-}$ are apparently sufficient to destabilize the uncomplexed planar conformer. Therefore both dimerization and complex formation perturb the local environment of the $NiUroP^{8-}$ affecting the conformation of the macrocycle.

The electronic structure of the macrocycle is also perturbed by the local environment of the porphyrin. Extended Hückel MO calculations performed on ruffled conformations of NiOEP[19] as well as INDO calculations performed on nonplanar bacteriochlorophyll[6] (BChl) suggest that nonplanar distortions of chromophores, which might be caused by the protein environment, can significantly affect the electronic structure of the macrocycle. Ruffling of NiOEP substantially destabilizes the $a_{1u}(\pi)$ and $a_{2u}(\pi)$ orbitals (by 0.13 and 0.06 eV, respectively) with respect to the relatively unaffected $e_g(\pi^*)$ orbitals, as shown by MO calculation comparing the triclinic A and tetragonal crystal structures.[19,20] The destabilization of the HOMOs in the nonplanar system results in a predicted red shift in the Soret and α absorption bands of 410 and 360 cm^{-1}, respectively. Such a shift is detected in the excitation profile of the ruffled and planar forms of NiOEP.[19] Barkigia et al.[6] have used the INDO method and the experimentally observed conformations of the two BChl b molecules that comprise the special pair of the reaction center of *Rhodopseudomonas viridis* to calculate substantial shifts in both the HOMOs and LUMOs of the nonplanar macrocycle.

Effects of Protein Binding on Macrocycle Conformation. The variation in the molecular orbital levels caused by nonplanar distortions of the macrocycle can be translated into modifications of the photochemical, redox,[6] and substrate (axial and π–π) binding properties. The degree of out-of-plane distortion of the macrocycle could be controlled by the protein site into which the porphyrin is bound; thus, nonplanar distortions of the macrocycle might provide a mechanism for protein control of the biological function of tetrapyrrole-containing active sites of proteins. For example, the sensitivity of heme proteins to perturbations of the local heme environment[28,29] may result, in part, from protein-induced distortions of the heme such as ruffling, puckering, or doming of the porphyrin.

An example of the effect of the protein local environment on macrocycle conformation is illustrated by the behavior of nickel protoporphyrin ($NiProtoP^{2-}$) when inserted into the active site of hemoglobin. In marked contrast with the behavior of $NiProtoP^{2-}$ incorporated into detergent micelles, the Raman spectrum of NiHbA in Figure 3 shows only the lines of a planar conformer at 1657 and 1519 cm^{-1} for ν_{10} and ν_3, respectively. These frequencies are within 1 cm^{-1} of the planar $NiProtoP^{2-}$ form observed in the micelles. Also, the line widths (9 ± 2 and 8 ± 2, respectively) are roughly the same as for the planar form of $NiProtoP^{2-}$. Thus, the planar species occurring in the protein is almost identical with the planar micellar form of $NiProtoP^{2-}$. However, in the protein the ruffled form corresponding to the solution ruffled species is entirely absent. Therefore, the effect of the protein environment on the macrocycle is similar to the effect of dimerization in that the ruffled conformation is destabilized. However, the protein effect is far greater, since none of the ruffled form is observed for NiHbA. Clearly, the active site of hemoglobin in the T quaternary structure strongly favors a planar macrocycle. The orientation of the proximal histidine, since it isn't bound, has little effect on the structure of the macrocycle in this case, implying that the nonbonding contacts in the heme pocket dictate the planar conformation of the macrocycle.

Figure 3 also shows the decomposition of the spectrum of the $NiProtoP^{2-}$-reconstituted α hemoglobin subunits ($Ni\alpha_{SH}$).[25] The ν_{10} region is resolved by the curve-fitting procedure into two lines with reasonable line widths, although there is no clear shoulder evident on the low-frequency side of the band. The decomposition into two reasonably broad lines is possible because the composite line shape for $Ni\alpha_{SH}$ is considerably broader than NiHbA. The frequency separation of the two components is also reasonable (3.0 and 4.7 cm^{-1} for ν_3 and ν_{10}, respectively) when compared with the separation for $NiProtoP^{2-}$ (4.6 and 6.3 cm^{-1}). On the basis of the ν_{10} shifts for NiOEP crystals, we estimate the dihedral angle of the ruffled forms to be 7° for $Ni\alpha_{SH}$ and 10° for $NiProtoP^{2-}$. Finally, the line widths for the ruffled components are marginally larger than those for the planar components. Therefore, we conclude that the $NiProtoP^{2-}$ molecule in the four-coordinate sites of the isolated $Ni\alpha_{SH}$-subunits exhibits either distinct planar and ruffled species or, alternatively, a broad distribution of conformers ranging from planar to slightly less ruffled than the ruffled species existing in CTAB micelles.

Effects of Macrocycle Conformation on Axial Ligand Affinity. The presence of a ruffled component for the α-chains is in marked contrast with NiHbA. This result may explain the noted[24,25,30-32] difference in affinity of the Ni ion for the proximal histidine for the Ni-reconstituted proteins. (Note the difference in relative intensities of the five- and four-coordinate lines of NiHbA and

(28) Shelnutt, J. A.; Rousseau, D. L.; Dethmers, J. K.; Margoliash, E. *Proc. Natl. Acad. Sci. U.S.A.* **1979**, *76*, 3865.
(29) Shelnutt, J. A.; Rousseau, D. L.; Dethmers, J. K.; Margoliash, E. *Biochemistry* **1981**, *20*, 6485.
(30) Manoharan, P. T.; Alston, K.; Rifkind, J. M. *J. Am. Chem. Soc.* **1986**, *108*, 7095.
(31) Shaanan, B. *J. Mol. Biol.* **1983**, *171*, 31.
(32) Case, D. A. In *Hemoglobin and Oxygen Binding*, Ho, C., Ed.; Elsevier Biomedical: New York, 1982; p 371.

Niα_{SH} in Figure 4.) The heme pocket of the Niα_{SH}-subunits is known to be more spacious,[30-32] allowing the nickel porphyrin in more active sites to ruffle. The ruffled conformers would be expected to have lower affinity for axial ligands because of their smaller equatorial Ni-N bond distance. Thus, in the more spacious heme pocket of the isolated α-subunits, less histidine is bound, even though when histidine is bound (five-coordinate sites) the Ni-histidine force constant is greater for Niα_{SH} than for NiHbA.[24,25] Apparently, by forcing the macrocycle into a planar conformation, the protein can increase ligand affinity. This suggests a possible mechanism for protein control of axial ligand affinity for nickel tetrapyrrole containing enzymes like methylreductase.

For derivatives of cofactor F_{430}, a nickel tetrapyrrole cofactor of the methylreductase enzyme, it is thought that axial ligation at the nickel(II) ion is controlled by the degree of planarity of the hydrocorphin macrocycle.[2-4,33] The great out-of-plane flexibility of this highly reduced porphyrin macrocycle suggests two possible mechanisms by which the protein might participate in the methyl-transfer reaction catalyzed by methylreductase. Because the size of the central core is determined by the macrocycle planarity, the protein can control the core size by varying planarity. In turn, by varying the core size, the protein forces can modify the ligand binding properties. Moreover, protein control over ruffling (and therefore core size) could be important for the redox function of methylreductase, since the Ni ion cycles between the large Ni(I) ion and small Ni(II) ion during the catalytic cycle.[34,35] Finally, protein control of macrocycle conformation may explain the large differences between the anomalous Raman spectrum of methylreductase and the spectra of the isolated F_{430} complexes.[4,33]

The crystal structure of native hemoglobin shows a domed macrocycle.[5] Therefore, the presence of a nonplanar conformation suggests a strained linkage through the proximal histidine that counters the strong forces holding the macrocycle into a planar conformation. The energy associated with the strain is stored not only in the Fe-histidine bond and its connection to the subunit interfaces but also the contacts with the pocket residues that oppose the nonplanar conformation.

In summary, the ruffling of nickel porphyrins in solution is shown to be a general effect for a variety of biologically significant porphyrin macrocycles. Environmental perturbations, such as π-π complex formation and dimerization, have a marked effect on the planarity of the macrocycle. Further, binding of nickel porphyrins to heme proteins has an even larger effect on macrocycle conformation and also a possible influence on chemical properties such as axial ligand affinity. It is clear from the present work that reconstitution of nickel porphyrins into heme proteins provides a new method of investigating nonbonding contacts in the active sites of proteins and of determining the importance of macrocycle distortions in the biological function of enzymes. It is also apparent from this study that the structural flexibility of the macrocycle might play an important role in understanding hemoprotein dynamics. This is especially true when the metal tetrapyrrole group experiences conformational distortions associated with biological function.

(33) Shiemke, A. K.; Shelnutt, J. A.; Scott, R. A. *J. Biol. Chem.* **1989**, *264*, 11236.
(34) Albracht, S. P. J.; Ankel-Fuchs, D.; Böcher, R.; Ellermann, J.; Moll, J.; van der Zwann, J. W.; Thauer, R. K. *Biochim. Biophys. Acta* **1988**, *955*, 86.
(35) Stolzenberg, A. M.; Stershic, M. T. *J. Am. Chem. Soc.* **1988**, *110*, 6391.

Structure and Basicity of Silyl Ethers: A Crystallographic and ab Initio Inquiry into the Nature of Silicon-Oxygen Interactions

Soroosh Shambayati,[†] James F. Blake,[‡] Scott G. Wierschke,[‡] William L. Jorgensen,*[,‡] and Stuart L. Schreiber*[,†]

Contribution from the Department of Chemistry, Harvard University, Cambridge, Massachusetts 02138, and Department of Chemistry, Purdue University, West Lafayette, Indiana 47907. *Received May 6, 1989*

Abstract: Analyses of the Cambridge Structural Database and results of ab initio molecular orbital calculations provide insights into the bond angle widening at oxygen and lowered basicity observed for silyl ethers in comparison to alkyl ethers. Common rationalizations for the phenomena based on interactions of oxygen lone pairs with silicon 3d orbitals and on steric effects do not find support. However, an alternative explanation that considers the detailed nature of the highest occupied molecular orbitals and concepts from Walsh diagrams accounts for the structural and chemical observations in a comprehensive manner.

The novel structural and chemical properties of silyl ethers are closely related. A striking geometrical observation is the widening of the bond angle about oxygen along the series, dimethyl ether ($\angle$C-O-C = 112°),[1] methoxysilane ($\angle$Si-O-C = 121°),[2] and disiloxane ($\angle$Si-O-Si = 144°).[3] This effect has been addressed in a variety of theoretical studies applying ab initio molecular orbital methods during the last ten years.[4-12] Attribution of the trend to mixing of oxygen lone-pair (n) and silicon 3d orbitals[2,3,13,14] has been challenged[4-7,11,12] though not entirely abandoned.[8] The dissenters have proposed enhanced steric effects and electrostatic

[†] Harvard University.
[‡] Purdue University.

(1) Blukis, V.; Kasai, P. H.; Meyers, R. J. *J. Chem. Phys.* **1963**, *38*, 2753.
(2) (a) Glidewell, C.; Rankin, D. W. H.; Robiette, A. G.; Sheldrick, G. M.; Beagly, B.; Freeman, J. M. *J. Mol. Struct.* **1970**, *5*, 417. (b) Blake, A. J.; Ebsworth, E. A. V.; Henderson, S. G. D.; Dyrbusch, M. *Acta Crystallogr.* **1988**, *C44*, 1 (CSD refcod: FUTZEZ).
(3) Almenningen, A.; Bastiansen, O.; Hedberg, K.; Traetteberg, M. *Acta Chem. Scand.* **1963**, *17*, 2455.
(4) Sauer, J.; Zurawski, B. *Chem. Phys. Lett.* **1979**, *65*, 587.
(5) Oberhammer, H.; Boggs, J. E. *J. Am. Chem. Soc.* **1980**, *102*, 7241.

0002-7863/90/1512-697$02.50/0